Pergamon

Cement and Concrete Research 32 (2002) 491–498

CEMENT AND CONCRETE RESEARCH

Corrosion measurements of steel reinforcement in concrete exposed to a tropical marine atmosphere

M.A. Pech-Canul*, P. Castro

Dept. de Fisica Aplicada, Cinvestav-IPN, Carretera Antigua a Progreso Km. 6, A.P. 73 Cordemex, CP97310, Mérida, Yucatán, Mexico

Received 17 April 2001; accepted 23 October 2001

Abstract

As part of a broad research program, reinforced concrete cylinders of different qualities were exposed to the marine atmosphere of North Peninsula of Yucatán. The cylinders were electrochemically monitored over a period of 56 months. The time for the onset of active corrosion was shorter for rebars in concretes with a high water-to-cement (w/c) ratio compared to that for rebars in low w/c ratio concrete. Results also indicate, as expected, that for equal periods of exposure, nominal corrosion current density (i_{corr}) values were generally higher for rebar in concrete with higher w/c ratio than those for rebar in low w/c ratio concrete. Analysis of the observed impedance spectra in terms of a modified Randles circuit (in which the ideal capacitor is replaced by a constant phase element (CPE)) appeared to be a reasonable approximation.

Keywords: Polarization resistance; Electrochemical impedance; Reinforced concrete; Chlorides; Corrosion rate

1. Introduction

Corrosion of steel reinforcement is the main cause of damage and early failure of reinforced concrete structures. In marine environments, the major cause of rebar corrosion has been identified as chloride-induced depassivation of the steel. Structures at the seashore of the Yucatán Peninsula (México) experience enhanced deterioration due to bad construction practices such as: the use of high water-to-cement (w/c) ratios, the use of aggregates that in most of the cases present an excess in fine particles (having as a consequence a higher consumption of water that impedes the correct cement hydration during the setting and curing of concrete), and the custom of making foundations in direct contact with the sedimentary layer of sand and seashell [1–3].

Most of the studies on the durability performance of concrete specimens exposed to chloride-containing environments have been carried out in short-term or accelerated laboratory tests. However, long-term tests performed under natural exposure conditions are expected to help in obtaining more conservative predictions of durability. Based on these considerations, a broad research program was initiated in which reinforced concrete specimens of different qualities (w/c ratios) and curing times were cast in the laboratory and then exposed to the tropical marine atmosphere of the Yucatán Peninsula for approximately 5 years. One of the objectives of this program was to establish the applicability of various electrochemical corrosion measurement techniques for assessment of long-term durability performance of reinforced concrete exposed to the direct action of a tropical marine atmosphere.

Corrosion potential (E_{corr}) monitoring, the linear polarization resistance (LPR) method and electrochemical impedance spectroscopy (EIS) were the techniques chosen for this study. These three techniques have been extensively used in laboratory investigations of the corrosion behavior of reinforced concrete exposed to chloride-containing environments [4–10]. Among them, EIS has the major advantage of providing the possibility of establishing a physical interpretation of the processes involved. Taking into account that, for large structures, the polarization behavior of reinforcement becomes complicated due to problems of signal confinement [11–16], test specimens of small dimensions were made, with a physical configuration similar to that used by other authors in laboratory EIS investigations of reinforcing steel in concrete [8,9].

---

* Corresponding author. Tel.: +52-99-812960x250; fax: +52-99-812917.

E-mail address: max@mda.cinvestav.mx (M.A. Pech-Canul).

PII: S0008-8846(01)00713-X

This paper focuses on checking the suitability of E_{corr}, LPR and EIS measurements for monitoring steel reinforcement corrosion throughout 56 months of direct specimen exposure to a tropical marine atmosphere. Results of such corrosion measurements obtained for specimens with 7 days of curing and a range of w/c ratios are described and compared.

2. Experimental procedure

Ordinary Portland Cement (Type I, ASTM-C-150) concrete was used. The coarse aggregate was crushed limestone of common use in the Yucatán Peninsula. The reinforcement consisted of standard type A-615, grade 60, No. 3 steel bars, used in the as-received condition. Fig. 1 shows a sketch of the cylindrical specimen configuration used in this investigation. Each specimen contained an embedded solid-state reference electrode (RE), which consisted of a segment of 3-mm-diameter activated titanium rod (ATR) of a type used successfully in similar investigations [17,18].

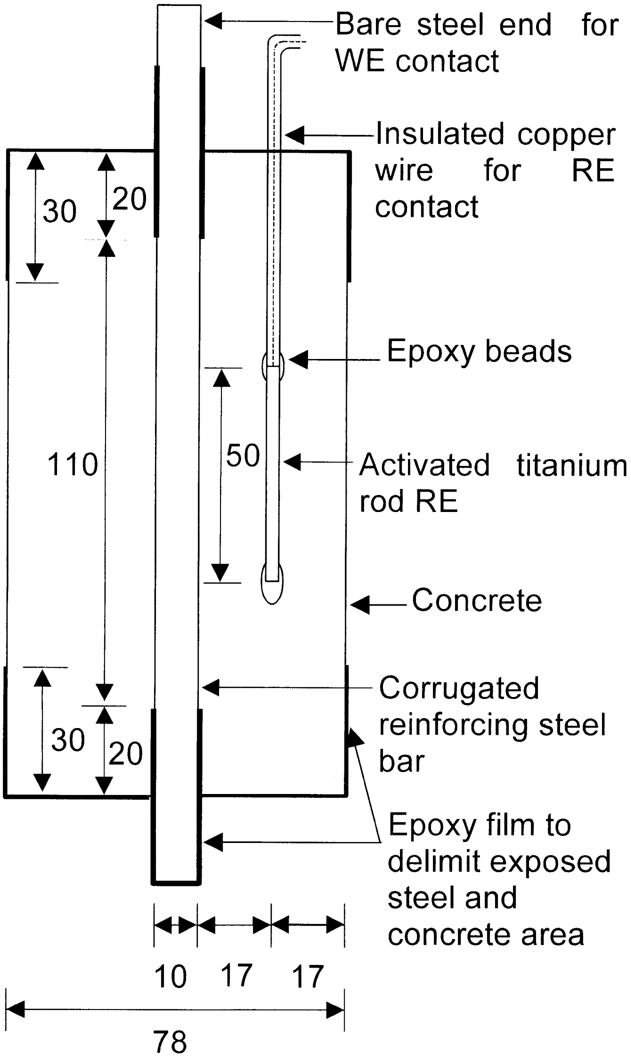

Fig. 1. Sketch of the specimen used (all dimension in mm).

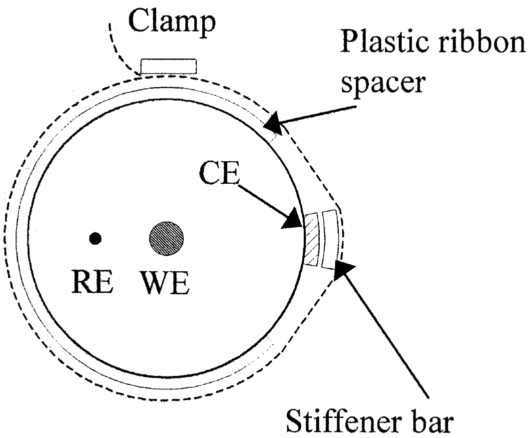

Fig. 2. Schematic showing the cell configuration.

For the corrosion tests reported in this paper, duplicate specimens of reinforced concrete having w/c ratios of 0.70, 0.50 and 0.46 were used. The curing time was 7 days in all cases. A parallel set of concrete cylinders was cast, without reinforcement, for chloride penetration studies. The ends of these specimens were sealed with epoxy in order to have just a radial penetration of chlorides. As indicated in detail elsewhere, a slice was cut on each cylinder, and the necessary powders for chloride determination were obtained from it by drilling [3].

The plain and reinforced concrete specimens were exposed to natural weathering in the marine atmosphere of the Port of Progreso, located on the coast of the Yucatán Peninsula (21°18′N, 89°39′W), which is characterized as a tropical humid climate [19–21]. The rack on which the specimens were exposed (in a vertical position) was located 50 m from the shoreline.

Electrochemical measurements were performed using the cell configuration of Fig. 2, where the working electrode (WE) was the reinforcing bar and the counter electrode (CE) was a single 15-mm-wide strip of elastomer running along the entire exposed concrete length. The strip was pressed longitudinally on the concrete surface using a stiff contoured metal bar that was fastened easily to the cylinder by two worm-thread hose clamps. Plastic ribbon spacers prevented the metal clamps from electric contact with the concrete surface. Such configuration was shown to provide more reproducible results compared to the typical configuration in which the CE surrounds the entire cylinder surface [22]. Electrode potentials were measured by means of a high impedance voltmeter and were always calibrated vs. the saturated calomel electrode (SCE).

LPR and EIS measurements were carried out with a commercial corrosion monitoring system. LPR measurements were conducted by varying the potential 10 mV (starting from the rest potential) in the negative direction, at a scan rate of 0.06 mV/s. EIS measurements were performed using a 10-mV amplitude sine wave signal in the frequency range between 0.1 mHz and 1 kHz with five points per decade.

3. Results and discussion

3.1. DC measurements

Fig. 3 shows the typical corrosion potential (E_{corr}) behavior, as a function of exposure time, of rebars in concrete cylinders with w/c ratios of 0.46, 0.50 and 0.70. The initial potential was about − 100 mV vs. SCE. Starting on the third month of exposure, potential fluctuations took place for the reinforcement within the three concrete mixes, with a clear trend towards more negative values. For comparison, horizontal lines were included at − 143 and − 293 mV, corresponding to the empirical criteria for the probability of corrosion used in ASTM C 876. Starting at approximately 6 months of exposure, potentials of reinforcing steel were indicative of corrosion likelihood in the three concrete mixes.

The values of i_{corr} corresponding to rebars in the three concrete mixes are presented in Fig. 4 as a function of exposure time. They were calculated from the polarization resistance values using a Stern–Geary constant of 26 mV [23]. Starting with values in the order of 0.01 μA/cm^2 corresponding to steel in the passive condition [24,25], there was a tendency of i_{corr} to increase, until a roughly constant value for each w/c ratio was achieved after ~36 months. Following the criteria suggested by Andrade et al. [26], it would appear that the time for initiation of active corrosion (when i_{corr} reached a value of 0.2 μA/cm^2) was shorter for concrete cylinders with a higher w/c ratio, compared to that for low w/c ratio concrete. This behavior has also been observed by other authors [27,28] and is consistent with the experimental data of chloride concentration at the rebar surface as a function of time given in Fig. 5. A horizontal line corresponding to the chloride threshold level (e.g. a value within the typical range 0.2–0.4 wt.% cement [29–31]) would intersect first the curve for w/c = 0.70, then the curve for w/c = 0.50 and lastly the curve for w/c = 0.46. Fig. 5 also shows that for a given exposure period, the chloride concentration at the rebar level is higher for concrete with a high w/c ratio, compared to that with a low w/c ratio. Such behavior can roughly be explained by the findings of other authors, indicating that the diffusivity of chloride ions through concrete is usually higher for poor quality concrete compared to that for good quality concrete [28,32–37].

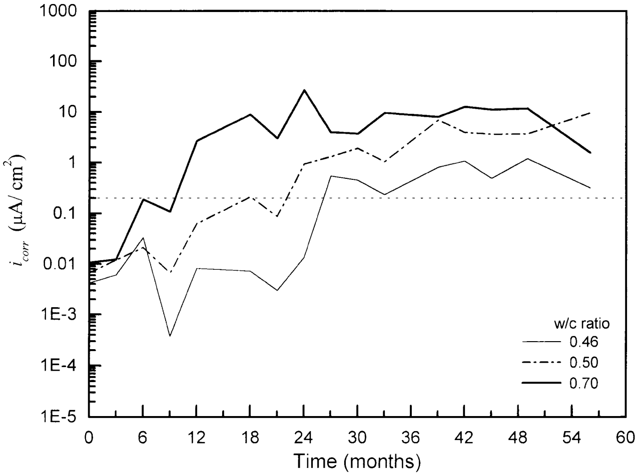

Fig. 4. Evolution of nominal corrosion current density as a function of exposure time for specimens with different w/c ratios.

Fig. 4 also shows that for equal periods of exposure to the tropical marine atmosphere (after the first 6 months),

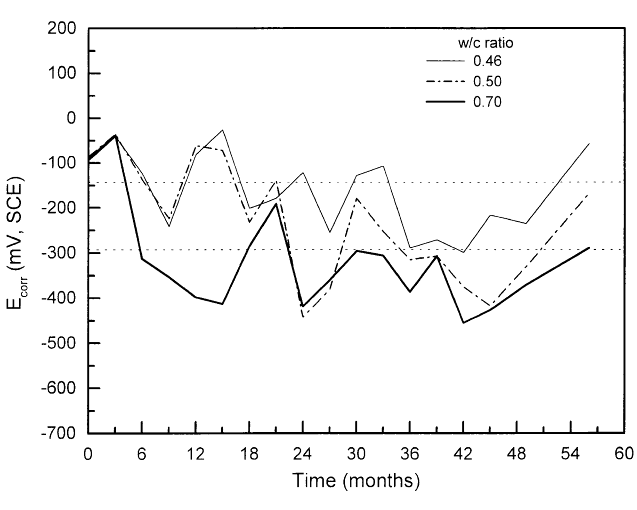

Fig. 3. Corrosion potential as a function of exposure time for specimens with different w/c ratios.

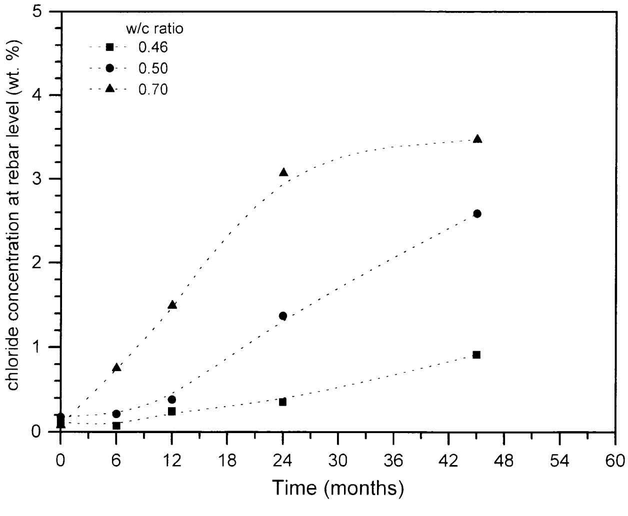

Fig. 5. Chloride concentration at the surface of reinforcing steel as a function of exposure time for specimens with different w/c ratios.

Table 1
Comparison of gravimetric vs. estimated weight loss of steel bars in the three concrete mixes at the end of the exposure period of 56 months

w/c Ratio	Gravimetric (mg/cm^2)	Estimated from area under i_{corr} vs. time curve (mg/cm^2)
0.46	58.8	16.8
0.50	172.7	138.8
0.70	643.3	544.0

i_{corr} values were generally higher for reinforcement within concretes having higher w/c ratios than those for low w/c ratio concrete. This behavior is not surprising and is in agreement with that reported by other authors [10,36,38,39]. It is corroborated by weight loss data (Table 1) for rebars in the three concrete mixes after the total exposure time of 56 months. As a comparison, Table 1 presents the weight loss resulting from the total area under the i_{corr} vs. time of exposure curve, and application of Faraday's law. The actual and estimated weight losses seem to correlate well, thus substantiating the validity of nondestructive electrochemical assessment of reinforcing steel corrosion.

3.2. EIS measurements

Fig. 6 shows the typical impedance behavior observed after 24 months of exposure for cylinders with w/c ratios of 0.46, 0.50 and 0.70. Fig. 7 shows the impedance spectra obtained for the cylinders with w/c ratios of 0.46 and 0.50 after an exposure period of 56 months. Each of the impedance diagrams in Figs. 6 and 7 exhibits two features: a semicircle with its center lying below the real impedance axis (~1 kHz–10 mHz frequency range), and a low frequency (LF) arc (frequency range below ~10 mHz), which does not converge to the real impedance axis even with frequencies down to ~0.1 mHz.

The depressed semicircle effect suggests a nonideal behavior of the capacitance C. For the purpose of assignment of such feature to a physical phenomena, a rough estimation of C can be made from the modulus of the

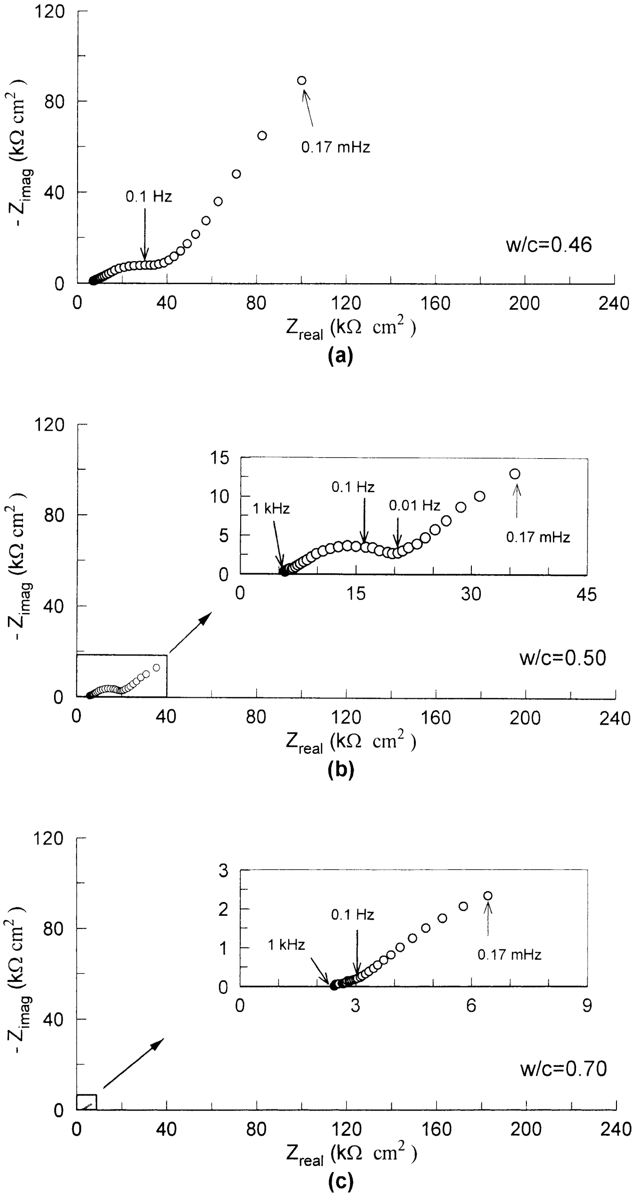

Fig. 6. Electrochemical impedance diagrams for specimens with different w/c ratios after an exposure time for 24 months.

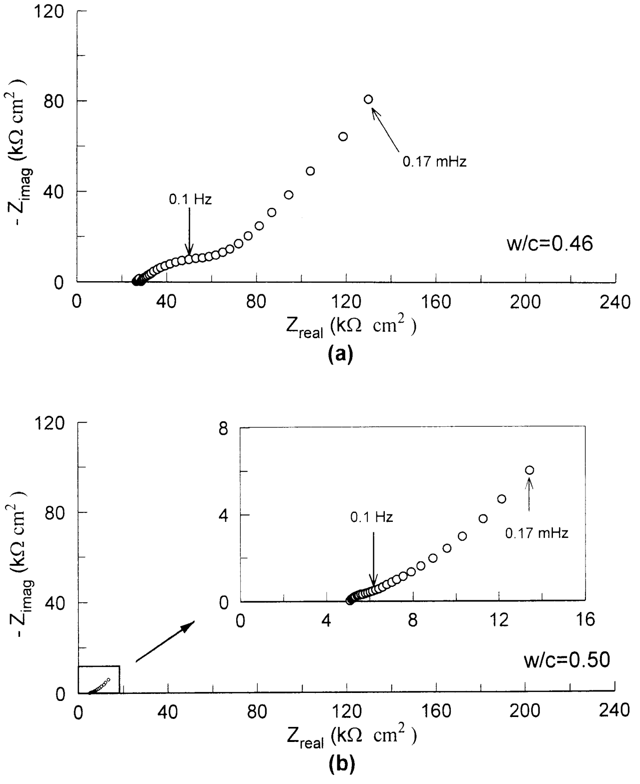

Fig. 7. Electrochemical impedance diagrams for specimens with different w/c ratios after an exposure time of 56 months.

complex capacitance at a frequency f^*, corresponding to the maximum value of the imaginary component

$$C = \left| -\frac{j}{2\pi f^* + Z(f^*)} \right|. \tag{1}$$

The average value of C obtained in this way for all the impedance diagrams in Figs. 6 and 7 was $\sim 100\ \mu F/cm^2$. This is a reasonable order of magnitude for a double-layer capacitance (C_{dl}) [40]. Thus, such semicircle might be due to the parallel combination of C_{dl} with the charge transfer resistance (R_{ct}).

Assuming that the LF arc is part of a second semicircle, a rough estimation of its capacitance, using Eq. (1) at the lowest test frequency (0.17 mHz), gives values ranging from 7×10^{-3} to 1×10^{-1} F/cm^2 for specimens exposed 24 months to the marine atmosphere. Large capacitance values and relaxation frequencies in the millihertz range have been ascribed by other authors to the response of a product layer [5,41] or the response of the Fe(II) $\Longleftrightarrow$ Fe(III) redox couple produced in oxide layers [42–44]. Since almost-perfect semicircles in the complex impedance plane would be expected for these two electrode-related features, it is unlikely that the LF arc corresponds to any of them because it exhibits a slope close to 45° in all the impedance diagrams of Figs. 6 and 7. Fig. 8 exemplifies (with the impedance data for the specimen with w/c = 0.50, after 24 months of exposure) that in the LF region the real and imaginary impedances are almost inversely proportional to the square root of the frequency. These observations suggest another possible mechanism: a diffusion process [4,5,45,46]. The common assumption is that such process corresponds to oxygen diffusion; however, not enough experimental evidence has been produced so far to verify such assumption. Nevertheless, based on the similarities of the observed impedance response with that reported recently by Feliu et al. [45], the impedance spectra in Figs. 6 and 7 were modeled, as a first approximation, by a modified Randles equivalent circuit (Fig. 9). In such circuit, the nonideal behavior of the capacitance is represented by a constant phase element (CPE). The impedance of the CPE is usually given by (Eq. (2)) [47]:

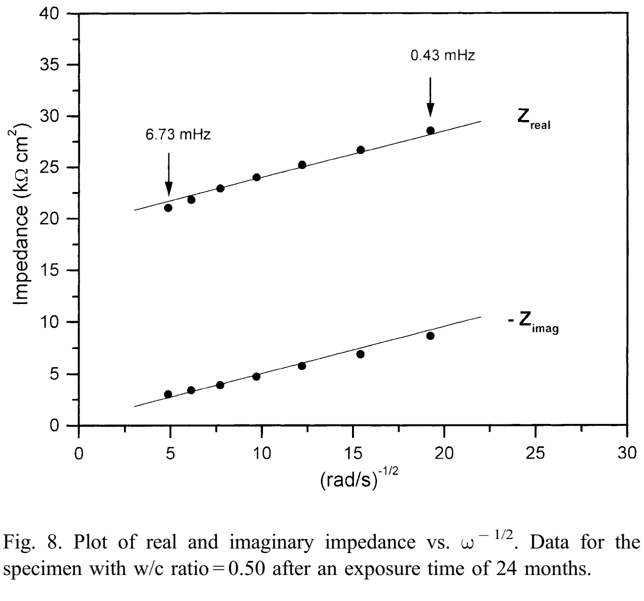

Fig. 8. Plot of real and imaginary impedance vs. $\omega^{-1/2}$. Data for the specimen with w/c ratio = 0.50 after an exposure time of 24 months.

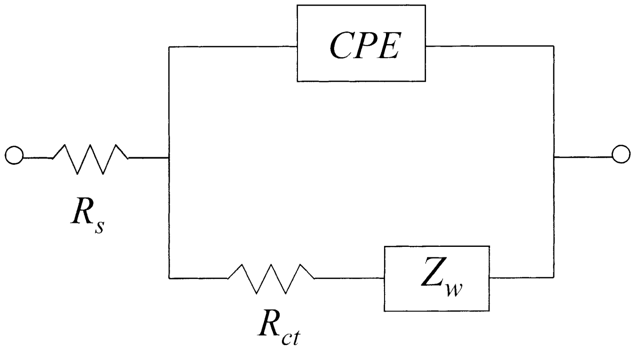

Fig. 9. Randles circuit modified with a CPE. R_s: ohmic resistance; R_{ct}: charge transfer resistance; Z_W: Warburg impedance.

$$Z_{CPE} = \frac{1}{Y_o(j\omega)^n} \tag{2}$$

where the exponent n provides information about the degree of nonideality in capacitive behavior, Y_o is the base admittance, $j = \sqrt{-1}$ and ω is the angular frequency. The diffusional component is represented by the Warburg impedance, Z_W (Eq. (3)) [47],

$$Z_W = \sigma(1-j)\omega^{-1/2} \tag{3}$$

where σ is known as the Warburg coefficient. For a mass transport controlled cathodic reaction, σ is related to the diffusion coefficient D through the following relationship [47]

$$\sigma = \frac{\beta_c}{\nu F C_s \sqrt{2D}} \tag{4}$$

where β_c is the Tafel coefficient, ν is the number of transferred electrons, F is the Faraday constant and C_s is the surface concentration of the electroactive species.

3.2.1. Equivalent circuit analysis

The observed spectra were analyzed using the circuit in Fig. 9, finding the model parameters that produced the best fit of the experimental data using a commercial software package [48]. A reasonable good agreement between the fit and experimental frequency responses was obtained, as exemplified in Fig. 10 for the reinforced concrete with w/c = 0.50 after 24 months of exposure. Table 2 presents the results of the equivalent circuit analysis for all the impedance spectra in Figs. 6 and 7. The electrical resistivity of concrete is generally decreased by a higher w/c ratio, since wider pores (high w/c) allow easier movement of current carrying ions [49]. Thus, as expected, the electrolyte resistance (R_s) values decreased for specimens with higher w/c ratios. The low n values in Table 2 were consistent with significant depression of the impedance diagrams in the complex impedance plane. Although CPE behavior has been often encountered for steel in concrete [40,45,50,51], a detailed description of its physical origin has not been given so far. Such task is beyond the scope of this paper. Nevertheless, the CPE parameters were used to estimate values of the apparent interfacial capacitance C_{app}, according to the relationship $C_{app}=(Y_o R_{ct})^{1/n}/R_{ct}$. The C_{app} values increased with increasing values of the w/c ratio, probably due to roughening of the surface (because corrosion rate for rebar in high w/c ratio concrete was higher than that for rebar in low w/c ratio concrete).

Table 2 shows that the R_{ct} values decreased for increasing values of the w/c ratio. Assuming that R_{ct} is inversely proportional to i_{corr}, the R_{ct} values (for 24 and 56 months of exposure) would indicate, in agreement with the results of DC measurements, that i_{corr} increases with w/c ratio. i_{corr} values estimated from the R_{ct} values using a Stern–Geary constant of 26 mV were in reasonable good agreement with those in Fig. 4, except for one case (w/c = 0.46, 24 months of exposure) in which the i_{corr} estimated with the LPR method was about two orders of magnitude lower than that estimated with EIS. Such discrepancy was probably due to uncertainties typical of electrochemical measurements in passive systems [52]. After 2 years of exposure to the marine atmosphere, the reinforcement in the concrete specimen with the highest quality (w/c = 0.46) was near the transition from passive to active behavior.

Regarding the diffusional process in the LF region, the estimation of D from Eq. (4) and the σ values in Table 2 would, in principle, help in deciding whether it is reasonable or not to ascribe the electroactive species to oxygen. However, such check up cannot be accomplished since the available results do not provide means of determining the corresponding C_s values. Nevertheless, it is interesting to note in Table 2 that the σ values decreased for increasing w/c ratios. Taking into account the inverse proportionality between σ and the square root of D, and also the observation that in concretes of different qualities, the oxygen diffusion coefficient increases with w/c ratio [53–55], the observed correlation between σ and w/c ratio might be considered a qualitative indication that the electroactive species is oxygen. It is evident that to verify the hypothesis that the LF arc is due to oxygen diffusion, specific laboratory tests and a more rigorous modeling would be needed. For instance, Andrade et al. [56] have shown with cathodic polarization tests that the availability of oxygen at the rebar surface in concrete is controlled by pore water saturation. Thus, EIS investigations using specimens with different levels of moisture saturation of the concrete pores are expected to provide useful mechanistic information for this purpose.

Table 2
Parameters from equivalent circuit analysis of EIS results

	w/c Ratio (24 months)			w/c Ratio (56 months)	
	0.46	0.50	0.70	0.46	0.50
R_s (kΩ cm^2)	8.19	6.3	2.5	28.3	5.16
Y_o (kΩ^{-1} cm^{-2} s^n)	0.01834	0.04874	0.8171	0.032	0.692
n	0.549	0.542	0.52	0.54	0.525
R_{ct} (kΩ cm^2)	27.63	14.87	0.87	36	2.47
C_{app} (μF/cm^2)	10.0	37.0	596.0	36.0	1124.0
σ (kΩ cm^2 s$^{-1/2}$)	2.37	0.44	0.1	2.08	0.182

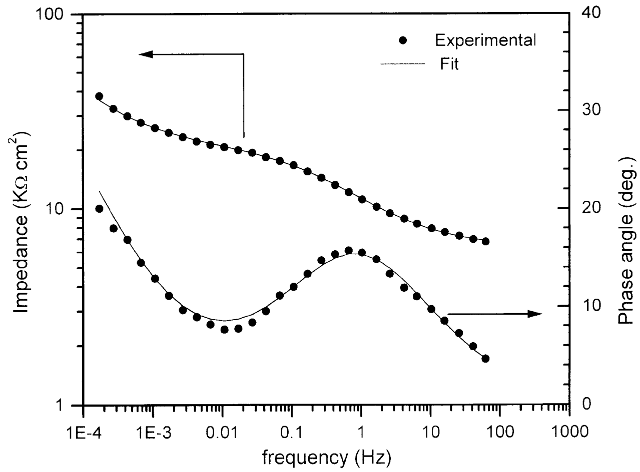

Fig. 10. Comparison between experimental data and best fit to the model represented by the equivalent circuit in Fig. 9. The data correspond to the specimen with w/c ratio = 0.46 after 24 months of exposure.

The R_{ct} values obtained from the fit process seem to be useful in the characterization of the degree of rebar corrosion. Thus, even when the available results give only a qualitative indication that the LF arc may be ascribed to oxygen diffusion, the simple model used to analyze the impedance spectra still provides a reasonable approximation for this study.

To sum up, the results of E_{corr} monitoring, LPR and EIS show good agreement and suggest that these techniques can actually be used together to monitor the corrosion development of reinforced concrete specimens exposed directly to the marine atmosphere. More negative values of E_{corr} were generally associated with larger values of i_{corr} determined by both LPR and EIS. The results show that in the aggressive marine atmosphere of the Yucatán Peninsula, the poorest performance was that of the reinforcing steel in concrete with a w/c ratio of 0.70 where active corrosion of the rebar started as early as ~6 months of exposure. The best performance was that of reinforcing steel in concrete with a w/c ratio of 0.46, for which a low level of corrosion activity was detected starting at about 2 years.

4. Conclusions

- The three electrochemical techniques used (E_{corr} monitoring, LPR and EIS) show good agreement in the detection of chloride-induced corrosion for reinforcing steel in concrete exposed to a tropical marine atmosphere.
- In agreement with chloride penetration data, the i_{corr} values (determined by both LPR and EIS) suggest, as expected, that the corrosion initiation time for rebars

in the three concrete mixes tested in this work followed the sequence: w/c ratio of 0.7 < w/c ratio of 0.5 < w/c ratio of 0.46.

- Results indicate, as expected, that for equal periods of exposure, i_{corr} values were generally higher for rebar in concrete with higher w/c ratio than those for rebar in low w/c ratio concrete.
- The evaluation of the charge transfer resistance from the analysis of the observed impedance spectra with a modified Randles circuit (in which the ideal capacitance is replaced by a CPE), appears to be reasonably appropriate.
- A correlation between σ and w/c ratio was observed, which was considered as a qualitative indication that the electroactive species in the cathodic reaction is oxygen.

Acknowledgments

The authors acknowledge partial support from the Centro de Investigación y Estudios Avanzados (CINVESTAV) and the Consejo Nacional de Ciencia y Tecnología (CONACYT) through contracts A9109, 2186 PA, and F051 I9110.The authors are grateful to professor Alberto A. Sagüés (University of South Florida) for the helpful discussions. We also wish to thank Ms. Mercedes Balancán for the technical assistance.

References

[1] P. Castro, The atmospheric corrosion performance of reinforced concrete in the Peninsula of Yucatán, México. A review, Corros. Rev. 17 (5) (1999) 333–382.

[2] P. Castro, L. Maldonado, R. Castillo, M. Balancán, M. Echeverría, Relationships between a potential mapping and a chloride penetration study in a public building at the seashore of the Gulf of México (in Spanish) 1st NACE Latin-American Region Corrosion Congress, Maracaibo (p. 1/94104).

[3] P. Castro, L. Maldonado, Initial efforts to evaluate the corrosion problems in the infrastructure of the mexican southeast coastal zones, in: V. Chaker (Ed.), Innovative Ideas for Controlling the Decaying Infrastructure, NACE International Book Pub., Houston, 1995, pp. 119–136.

[4] D.G. John, P.C. Searson, J.L. Dawson, Use of AC impedance technique in studies on steel in concrete in immersed conditions, Br. Corros. J. 16 (2) (1981) 102–106.

[5] B.B. Hope, J.A. Page, K.C. Ip, Corrosion rates of steel in concrete, Cem. Concr. Res. 16 (5) (1986) 771–781.

[6] L. Hachani, J. Carpio, C. Fiaud, A. Raharinaivo, E. Triki, Steel corrosion in concretes deteriorated by chlorides and sulphates: Electrochemical study using impedance spectrometry and "steppind down the current" method, Cem. Concr. Res. 22 (1992) 56–66.

[7] L. Hachani, E. Triki, J. Grandet, A. Raharinaivo, Comparing the steel–concrete interface state and its electrochemical impedance, Cem. Concr. Res. 26 (2) (1996) 253–266.

[8] L. Lemoine, F. Wenger, J. Galland, Study of the corrosion of concrete reinforcement by electrochemical impedance measurement, in: N.J. Berke, V. Chacker, D. Whiting (Eds.), Corrosion Rates of Steel in Concrete, ASTM STP 1065, American Society for Testing and Materials, Philadelphia, 1990, pp. 118–133.

[9] C. Andrade, L. Soler, C. Alonso, X.R. Novoa, M. Keddam, The importance of geometrical considerations in the measurement of steel corrosion in concrete by means of ac impedance, Corros. Sci. 37 (12) (1995) 2013–2023.

[10] P. Gu, J.J. Beaudoin, M. Zhang, V.M. Malhotra, Performance of steel reinforcement in portland cement and high-volume fly ash concretes exposed to chloride solution, ACI Mater. J. 96 (5) (1999) 551–558.

[11] S. Feliu, J.A. González, V. Feliu Jr., M.C. Andrade, Confinement of the electrical signal for in situ measurement of polarization resistance in reinforced concrete, ACI Mater. J. 87 (5) (1990) 457–460.

[12] D.D. Macdonald, M. Urquidi-Macdonald, R.C. Rocha-filho, Y. El-tantawy, Determination of the polarization resistance of rebar in reinforced concrete, Corrosion 47 (5) (1991) 330.

[13] K. Matsuoka, H. Kihira, S. Ito, T. Murata, Corrosion monitoring for reinforcing bars in concrete, in: N.S. Berke, V. Chaker, D. Whiting (Eds.), Corrosion Rates of Steel in Concrete, ASTM STP 1065, American Society for Testing and Materials, Philadelphia, 1990, pp. 103–117.

[14] J. Flis, S. Sabol, H.W. Pickering, A. Sehgal, K. Osseo-Asare, P.D. Cady, Electrochemical measurements on concrete bridges for evaluation of reinforcement corrosion rates, Corrosion 49 (7) (1993) 601.

[15] K.R. Gowers, S.G. Millard, On-site linear polarization resistance mapping of reinforced concrete structures, Corros. Sci. 35 (5–8) (1993) 1593.

[16] P. Rodriguez, E. Ramirez, J.A. Gonzalez, Methods for studying corrosion in reinforced concrete, Mag. Concr. Res. 46 (167) (1994) 81–90.

[17] P. Castro, A.A. Sagüés, E.I. Moreno, L.A. Maldonado, J. Genescá, Characterization of activated titanium solid reference electrode for corrosion testing of steel in concrete, Corrosion 52 (8) (1996) 609–617.

[18] A.A. Sagüés, H.M. Pérez-Duran, R.G. Powers, Corrosion performance of epoxy-coated reinforcing steel in marine substructure service, Corrosion 47 (11) (1988) 884–893.

[19] L. Véleva, P. Castro, G. Hernández-Duque, M. Schorr, The corrosion performance of steel and reinforced concrete in a tropical humid climate. A review, Corros. Rev. 16 (3) (1998) 235–284.

[20] P. Castro, L. Véleva, M. Balancán, Corrosion of reinforced concrete in a tropical marine environment and in accelerated tests, Constr. Build. Mater. 11 (2) (1997) 75–81.

[21] L. Maldonado, L. Véleva, Corrosivity category maps of a humid tropical atmosphere: The Yucatan Peninsula, Mexico, Mater. Corros. 50 (5) (1999) 261–266.

[22] M.A. Pech-Canul, A. Sagües, P. Castro, Influence of counter electrode positioning on the solution resistance in impedance measurements of reinforced concrete, Corrosion 54 (8) (1998) 663–667.

[23] C. Andrade, J.A. González, Quantitative measurements of corrosion rate of reinforcing steels embedded in concrete using polarization resistance measurements, Werkst. Korros. 29 (1978) 515–519.

[24] C. Andrade, C. Alonso, S. Feliu, J.A. González, Applications of corrosion rate values, in: A. Blankvoll (Ed.), Proceedings of the International Conference on Repair of Concrete Structures, From Theory to Practice in Marine Environment, Norwegian Road Res Lab., Svolvaer, 1997, pp. 365–374.

[25] P. Rodriguez, J.A. González, Use of the coulostatic method for measuring corrosion rates of embedded metal in concrete, Mag. Concr. Res. 46 (167) (1994) 91–97.

[26] C. Andrade, M.C. Alonso, J.A. González, An initial effort to use the corrosion rate measurements for estimating rebar durability, in: N.S. Berke, V. Chaker, D. Whiting (Eds.), Corrosion Rates of Steel in Concrete, ASTM STP 1065, American Society for Testing and Materials, Philadelphia, 1990, pp. 29–37.

[27] Rasheeduzzafar, S.S. Al-Saadoun, A.S. Al-Ghatani, F.H. Dakhil, Effect of tricalcium aluminate content on corrosion of reinforcing steel in concrete, Cem. Concr. Res. 20 (5) (1990) 723–738.

[28] P. Arora, B.N. Popov, B. Haran, M. Ramasubramanian, S. Popova,

A.H.S. El-Busaidy, Corrosion initiation time of steel reinforcement in a chloride environment — a one dimensional solution, Corros. Sci. 39 (4) (1997) 739–759.

[29] G.K. Glass, N.R. Buenfeld, The presentation of the chloride threshold level for corrosion of steel in concrete, Corros. Sci. 39 (5) (1997) 1001–1013.

[30] P.B. Bamforth, Chloride penetration and service life, Proceedings of Corrosion and Protection of Metals in Contact with Concrete, COST-509 Workshop (Sevilla).

[31] M. Thomas, Chloride thresholds in marine concrete, Cem. Concr. Res. 26 (4) (1996) 513–519.

[32] M. Maage, S. Helland, E. Poulsen, Ø. Vennesland, J.E. Carlsen, Service life prediction of existing concrete structures exposed to marine environment, ACI Mater. J. 93 (6) (1996) 602.

[33] R.K. Dhir, E.A. Byars, PFA concrete: Chloride diffusion rates, Mag. Concr. Res. 45 (162) (1993) 1–9.

[34] P.S. Mangat, B.T. Molloy, Chloride binding in concrete containing PFA, gbs or silica fume under sea water exposure, Mag. Concr. Res. 47 (171) (1995) 129–141.

[35] A.V. Saetta, R.V. Scotta, R.V. Vitaliani, Analysis of chloride diffusion into partially saturated concrete, ACI Mater. J. 90 (5) (1993) 441–451.

[36] C.M. Hansson, N.S. Berke, Chlorides in concrete, in: L.R. Robert, J.P. Skalny (Eds.), Pore Structure and Permeability of Cementitious Materials, Mater. Res. Soc. Symp. Proc., vol. 137, Materials Research Society, 1989, pp. 253–270.

[37] D.W. Hobbs, Aggregate influence on chloride ion diffusion into concrete, Cem. Concr. Res. 29 (12) (1999) 1995–1998.

[38] D. Baweja, H. Roper, V. Sirivivatnanon, Chloride-induced steel corrosion in concrete: Part 1. Corrosion rates, corrosion activity, and attack areas, ACI Mater. J. 95 (3) (1998) 207–217.

[39] D. Baweja, H. Roper, V. Sirivivatnanon, Chloride-induced steel corrosion in concrete: Part 2. Gravimetric and electrochemical comparisons, ACI Mater. J. 96 (3) (1999) 306–313.

[40] J. Flis, H.W. Pickering, K. Osseo-Asare, Interpretation of impedance data for reinforcing steel in alkaline solution containing chlorides and acetates, Electrochim. Acta 43 (12/13) (1998) 1921–1929.

[41] S.J. Ford, J.D. Chane, T.O. Mason, Assignment of features in impedance spectra of the cement-paste/steel system, Cem. Concr. Res. 28 (12) (1998) 1737–1751.

[42] C. Andrade, L. Soler, X.R. Novoa, Advances in electrochemical impedance measurements in reinforced concrete, Mater. Sci. Forum 192–194 (1995) 843–856.

[43] C. Andrade, P. Merino, X.R. Novoa, M.C. Pérez, L. Soler, Passivation of reinforcing steel in concrete, Mater. Sci. Forum 192–194 (1995) 891–898.

[44] S. Feliu, J.C. Galván, S. Feliu Jr., J.M. Bastidas, J. Simancas, M. Morcillo, E.M. Almeida, An electrochemical impedance study of the behavior of some pretreatments applied to rusted steel surfaces, Corros. Sci. 35 (5–8) (1993) 1351–1358.

[45] V. Feliu, J.A. González, C. Andrade, S. Feliu, Equivalent circuit for modelling the steel–concrete interface: I. Experimental evidence and theoretical predictions, Corros. Sci. 40 (6) (1998) 975–993.

[46] V. Feliu, J.A. González, C. Andrade, S. Feliu, Equivalent circuit for modelling the steel–concrete interface: II. Complications in applying the Stern–Geary equation to corrosion rate determinations, Corros. Sci. 40 (6) (1998) 995–1006.

[47] J.R. Macdonald (Ed.), Impedance Spectroscopy, Emphasizing Solid Materials and Systems, Wiley, New York, 1987.

[48] B.A. Boukamp, Equivalent Circuit University of Twente, Netherlands, 1989.

[49] R.B. Polder, P.B. Bamforth, M. Basheer, J. Chapman-Andrews, R. Jafar, M.I. Jafar, A. Mazzoni, E. Nolan, H. Wojtas, Reinforcement corrosion and concrete resistivity, in: Proceedings of the International Conference on Corrosion and Corrosion Protection of Steel in Concrete, Sheffield Academic Press (Sheffield).

[50] A.A. Sagüés, S.C. Kranc, E.I. Moreno, The time-domain response of a corroding system with constant phase angle interfacial component: Application to steel in concrete, Corros. Sci. 37 (7) (1995) 1097–1113.

[51] P. Gu, S. Elliott, R. Hristova, J.J. Beaudoin, R. Brousseau, B. Baldock, A study of corrosion inhibitor performance in chloride contaminated concrete by electrochemical impedance spectroscopy, ACI Mater. J. 94 (5) (1997) 385–395.

[52] J.A. González, A. Molina, M.L. Escudero, C. Andrade, Errors in the electrochemical evaluation of very small corrosion rates: I. Polarization resistance method applied to corrosion of steel in concrete, Corros. Sci. 25 (10) (1985) 917–930.

[53] K. Kobayashi, K. Shuttoh, Oxygen diffusivity of various cementitious materials, Cem. Concr. Res. 21 (1991) 273–284.

[54] O.E. Gjorv, O. Vennesland, A.H.S. El-Busaidy, Diffusion of dissolved oxygen through concrete, Mater. Perform., (12) (1986) 39–44.

[55] K. Tuuti, Corrosion of Steel in Concrete, Report CBI 10.4.82, Swedich Cement and Concrete Research Institute, Stockholm, 1982.

[56] C. Andrade, C. Alonso, A.M. García, Oxygen availability in the corrosion of reinforcements, Adv. Cem. Res. 3 (11) (1990) 127–132.